Hindawi
International Journal of Energy Research
Volume 2023, Article ID 4951589, 18 pages
https://doi.org/10.1155/2023/4951589

Research Article

A Comprehensive Technoeconomic and Environmental Evaluation of a Hybrid Renewable Energy System for a Smart Farm in South Korea

Karim Rabea,[1,2] **Stavros Michailos**,[3] **Godfrey T. Udeh**,[1] **Jiseon Park**,[4] **YongWoon Lee**,[4] **Seongil Kim**,[4] **Won Yang**,[4] **Kevin J. Hughes**,[1] **Lin Ma**,[1] **and Mohamed Pourkashanian**[1]

[1]*Energy 2050, Department of Mechanical Engineering, The University of Sheffield, Sheffield S3 7RD, UK*
[2]*Department of Mechanical Power Engineering, Faculty of Engineering, Tanta University, Tanta 31521, Egypt*
[3]*School of Engineering, Faculty of Science and Engineering, University of Hull, Hull HU6 7RX, UK*
[4]*Carbon Neutral Technology R&D Department, Korea Institute of Industrial Technology, Cheonan-si, Chungcheongnam-do 31056, Republic of Korea*

Correspondence should be addressed to Karim Rabea; kelamawy1@sheffield.ac.uk

Received 17 February 2023; Revised 20 June 2023; Accepted 24 June 2023; Published 14 July 2023

Academic Editor: Geng Chen

The farming sector like any other industry needs to be decarbonized. Hence, it is essential to meet the energy demands of the farms by adopting energy systems with a low-carbon footprint. Depending on the weather conditions, heating or cooling is needed. Within this context, this study presents a new hybrid renewable decentralized energy system that is designed to satisfy the requirements for heating, cooling, and electricity of a smart farm in South Korea. The under-investigation energy system comprises solar PV arrays, heat pumps, thermal energy storage tanks, and a wood pellet boiler. This study is the first to conduct an inclusive techno-enviroeconomic assessment of such a hybrid energy system by utilizing actual meteorological data on an hourly basis. This enables the model to be dynamic and facilitate accurate and reliable assessments. The modelling efforts have been performed in Aspen Plus and MATLAB to investigate the thermodynamic behaviour of the system. The investigation shows that the proposed system has achieved a daily average temperature of around 23.9°C inside the farm throughout the year with a standard deviation of 2.16°C. For the economic assessment, the levelized cost of energy has been selected as the main economic indicator, and this has been estimated at $0.218/kWh. It is found that the PV panels and the biomass boiler dominate the capital expenditures, and the biomass feedstock is the major contributor to the operating expenditures. Further, the proposed energy system reduces CO_2 emissions, by up to 88.94%, when compared to conventional fossil-based energy systems. The outcomes of this study represent a holistic evaluation for such a low-carbon hybrid energy system when applied to greenhouses in Korea and in similar locations.

1. Introduction

The globally unprecedented pace of climate change has introduced a new dimension to the generation and consumption of energy, and this has been exacerbated by the existing energy crisis. Therefore, most countries have attempted to accelerate their rate of implementing renewable and sustainable energy sources, since this is a very important and vital approach for all the world to reduce the reliance on fossil fuels. One pathway that is being explored to achieve this transition is encouraging, namely, the development of hybrid energy systems, especially from the use of the available local renewable sources, such as biomass and solar [1]. In addition, most governments have implemented several interesting policies that could incentivise the deployment of clean energy solutions. Some of these policies are presented in the form of investment grants, feed-in tariffs, feed-in premiums, and green energy credits [2]. One of the most interesting initiatives was the introduction of the concept of "prosumers of energy," which has opened the door

for the utilization of different clean and renewable energy sources [3, 4]. This can be in the form of hybrid energy systems, which introduce several ingenious strategies to improve the energy efficiency, such as the cogeneration of heating and electricity.

Recently, the agricultural sector in the Republic of Korea has been paying more attention to the mitigation of the GHG emissions, and this is believed to be possible to be attained through the employment of smart farms as a replacement to the traditional farms [5]. The aim of the smart farms is to achieve the prosumer concept, in which the energy is produced from the renewable sources and consumed on site. In addition, the excess energy is supplied to the grid or stored. However, the smart farms require high investment costs to meet the high energy demands which are mainly required for the heating purposes [6]. About 53.4% of the total energy consumed by the agricultural sector is devoted to the heating and cooling systems, where this demand is mainly covered by fossil fuels [7]. Therefore, the need to develop an efficient and cost-effective energy system based on renewable energy sources is necessary to meet the carbon neutralization targets [8, 9]. It is important to note that the agricultural sector in the Republic of Korea targets to achieve 4.8% of the total national targeted emission reduction of CO_2 [6]. This can be achieved by adopting different renewable energy sources in hybrid configurations.

It is important to note that the cogeneration of power and heat from the hybrid renewable energy systems can increase the efficiency and the reliability of such a system while maintaining low-carbon emissions. The photovoltaic power generation has evolved significantly over the recent years, and it has been proved to be suitable and reliable to produce energy over a long period of time [10]. Also, when it comes to the efficient heating equipment, the heat pumps are on top of the list for power-to-heat applications, with a high coefficient of performance (COP) that can reach over 6 as reported in [11]. The heat pumps can be distinguished by one of the two main types, ground-source heat pump (GSHP) and air-source heat pump (ASHP).

Many research studies have been conducted to evaluate the performance of the GSHP for greenhouse heating and cooling purposes. For instance, Chai et al. [12] investigated the performance of a GSHP for greenhouse heating as a replacement of the traditional coal- or gas-fired heating system in Beijing, China. The heat pump has proved its suitability to satisfy the heating load with an average COP of 3.87 at even lower daily heating cost than the gas-fired heater by an average of 10.15%. In addition, even though the GSHP was not cost-competitive against the coal-fired heater, the environmental impact should be taken into consideration. Similarly, Luo et al. [13] compared the thermoeconomic performance of a coal-fired heating system against a GSHP for greenhouse heating in China. The maximum thermal efficiency of the boiler was 68%, while the COP of the heat pump was 3.3 for cooling and 4.1 for heating, and this represents a high level of energy savings by the employment of the heat pump. Furthermore, the considered lifetime of the coal-fired boilers is short, 10 years vs. 20 years for the GSHP. This in turn favours the economic performance of the GSHP over its lifetime, where the average energy price was \$0.023/kWh and \$0.04/kWh for the cooling and heating, respectively, whereas for the coal-fired boiler, it was \$0.052/kWh. The significant difference between the COPs of the heat pumps and the thermal efficiencies of the conventional systems also implies high CO_2 emission reduction (CO_2ER). For instance, the heat pump has achieved an average reduction of 43.25% when compared to the coal-fired heating [12]. Interestingly, these high COPs favoured the economic and environmental performance, and this still can be observed for combined systems. In a study conducted in Japan by Zhou et al. [14], they showed that combining a GSHP with a fuel oil heater as a hybrid system for greenhouse heating can reduce the energy consumption by 22.8% and the CO_2 emissions by 35.5% when compared to the employment of only an oil heater.

The performance of the heat pump can be further improved by utilizing solar energy, which can be in the form of thermal energy or electrical energy. The solar thermal energy can be employed to heat the water or the air for the evaporator of the heat pump using the solar collectors [7, 15–18]. In order to evaluate this integration, Hassanien et al. [16] have investigated the feasibility of implementing a solar-assisted heat pump for the heating of a greenhouse in China. The integration was achieved by employing an evacuated tube solar collector with an efficiency of 49% to heat the water for the heat pump. Through this integration, the solar collector, by itself, has supplied more than 35% of the heat demand over one year. This represents the estimated energy savings over one year from this integrated system, which is mainly attributed to the contribution of the solar thermal energy that increases the COP of the heat pump [15].

Recently, in order to reduce the carbon footprint even further, the PV technology has been increasingly adopted for the power generation as well as for heating and cooling purposes through the integration with the heat pumps [10, 19]. For heating purposes, Russo et al. [20] compared the environmental impact of a GSHP powered by solar PV panels and the grid to an LPG-based heat generation system in Italy. It was found that the GSHP-PV combination has achieved a 50% emission reduction of CO_2 relative to the LPG-based heating. This can be even higher, up to 80%, when compared to an electricity-based heating system based in the Netherlands [21]. Also, for the PV-based combined heating and power system (CHP), Yildirim and Bilir [22] have evaluated the performance of such a system in a greenhouse by employing solar PV panels along with a GSHP to provide power and heat to the farm with low emissions in Turkey. The PV system has satisfied between 33.2% and 67.2% of the total energy demand during the summer months, but the net annual coverage ratio of the energy load by the solar PV panels varied between 86.6% and 104.5%.

It can be observed from the literature that integrating the solar energy with the heat pump represents a promising approach to mitigate the environmental impact of a greenhouse CHP system. However, there are several limitations on the performance of the solar energy systems (i.e., the collectors and the PV panels), which are mainly associated to

the weather condition. To overcome these limitations, the solar PV panels can be backed up by electricity from the grid to run the heat pump when applicable. In addition, the heat pump is commonly integrated with a boiler as a backup heat source to the solar collector, or as an alternative to the heat pump itself. In this regard, biomass-fuelled boilers are considered as carbon neutral systems, especially when the biomass is grown at a rate equivalent to, or more than, its consumption. The other advantage of biomass-based systems is their ability to run on several locally available biomass fuels [23]. Finally, the utilization of actual meteorological data is of paramount importance for carrying out accurate technoeconomic and environmental assessments [12].

In particular, in the Republic of Korea, a hybrid system of a hydrothermal heat pump and a wood pellet boiler has been investigated for greenhouse heating [24]. The hybrid system has achieved higher thermal efficiency and lower running cost than the pellet boiler alone. Also, when compared to the conventional fossil fuel boiler, the carbon emission has been reduced by up to 71% [24]. However, when the system is integrated with a solar water heater, lower energy efficiency has been estimated, and therefore, it was not cost-effective. This is due to the limited availability of heat during the winter season in Korea. On the other hand, the PV-based hybrid systems can represent a more suitable approach, especially during cold periods. In addition, another advantage of the PV-ASHP energy system is the ability to run the heat pump for the farms in rural areas (off the grid), and in case of the grid-connected PV systems, the surplus electricity can be exported to the grid.

To the best of our knowledge, there is no study on solar PV-ASHP hybrid systems for greenhouse heating in Korea. Also, the previous studies are time-constrained, as they consider only a few operational days of the year, and this represents a shortcoming in the economic and environmental assessment. In view of these, the present study is aimed at investigating the performance of a hybrid renewable energy system comprising PV solar panels coupled with ASHPs and a wood pellet boiler to supply the energy demand of a smart farm in the Republic of Korea. In order to evaluate the feasibility of such a system, a comprehensive technoeconomic and environmental investigation has been conducted. The model utilizes the onsite operating data of the farm along with the hourly based meteorological data that is obtained from the same location. The outcomes of this study can and do provide meaningful insights into the viability of such a hybrid energy system and how it can contribute to the transition of the agricultural sector towards renewable decentralized energy solutions in Korea and in similar locations. Further, due to the modularity of the individual energy components, the proposed energy system has great scalability potential.

2. System Description

The smart farm that is investigated is located at the Jeollanamdo Agricultural Research and Extension Services, 1508, Senam-ro, Sanpo-myeon, Naju-si, Jeollanam-do, Republic of Korea. Figure 1 shows a schematic overview of the farm in addition to examples of the cultivated crops in 2021. The farm's total area is 1,378 m^2 and the height is 4.2 m.

The under-investigation energy system is an integration of solar PV-powered heat pumps and a backup wood pellet boiler in order to improve the reliability of the system. The system conditions the air in the farm all year round, and hence, it operates in winter and summer modes. Throughout the year, the grid-connected solar PV system is the primary source of power, and it is used to operate the heat pumps, the water circulation circuit, and the fan coil units (FCUs). The PV panels operate throughout the whole year, regardless of how much the heat pump operates, while any deficiency or excessiveness of the solar power is backed up and balanced by the grid. In case of the absence of solar energy, the wood pellet boiler is engaged to satisfy the heat load of the smart farm; this is only necessary for the wintertime. When no heating or cooling is required by the greenhouse farm, all the energy from the solar PV panels is exported to the grid. The actual layout of the piping configuration for the smart farm energy system is presented in Figure 2.

The layout exhibits the configuration of the energy system that is planned to be commissioned. The smart farm is designed to be sectioned to two planting areas (60%, i.e., 1st smart farm, and 40%, i.e., 2nd smart farm) to host different agricultural crops, and hence, the FCUs are distributed accordingly to sets of 15 and 10 units, respectively. Also, it shows the piping network as well as the temperature-based control valves that are employed to control the temperature on the heat pumps and the storage tank. For example, when the heat pumps produce hot water (over 50°C) and it is circulated between the water storage tank and the heat pump, the temperature control valve will open to control the water temperature by increasing the amount of the cold return water. The energy system is designed to have 5 heat pumps and a wood pellet boiler, and their specifications, as provided by the suppliers, are presented in Table 1.

The combined system has been modelled in Aspen Plus and MATLAB. Aspen Plus is a Fortran-based process modelling software package that has been extensively deployed to model various processes, including energy systems. It has an inclusive database of chemical, thermal, and physical properties of several compounds and holds a library of commonly used operation blocks. The developed model will inform and dictate the farm's operational strategies.

3. Model Development and Methods

3.1. Process Modelling Approach. For the solar PV panels, the hourly based simulation of the power generation from the PV module can be obtained by the following equation [25–27]:

$$P_{\mathrm{PV}}(t) = P_{\mathrm{STC}}\left[\frac{G_h(t)}{G_{\mathrm{STC}}}\left(1 + \frac{\alpha}{100}\left(T_c(t) - T_a(t)\right)\right)\right]F_{\mathrm{loss}}, \quad (1)$$

where P_{STC} (W) is the module maximum power at standard test conditions, G_h and G_{STC} (W/m^2) are the hourly global solar radiation and the solar radiation at the test conditions,

(a) (b) (c) (d)

Figure 1: Schematic of the smart farm: (a) drawing, (b) image of the actual farm, (c) paprika and tomato, and (d) apple and mango.

and α (%/°C) is the temperature coefficient. T_c and T_a (°C) are the cell and ambient temperatures, respectively, and F_{diss} (-) is a loss factor that accounts for the power dissipation due to dirt, wires, module mismatch, and other losses. The site and the required weather data are acquired from a station that is located in the city of Naju, Korea. All the weather data can be found in the Supplementary Material (available here). The cell temperature T_c (°C) is obtained from the following expression [25, 28]:

$$T_c(t) = T_a(t) + \left(\frac{\text{NOCT} - 20}{0.8}\right)\frac{G_h(t)}{G_{\text{STC}}}, \tag{2}$$

where NOCT (°C) is the nominal operating cell temperature and T_a (°C) is the ambient temperature. The specifications of the adopted PV panels are shown in Table 2.

The power produced from the PV array is utilized to operate the heat pumps, which are simulated along with the wood pellet boiler in Aspen Plus. The five heat pumps are simulated as a single heat pump with the overall cooling capacity of 325 kW_{th}. In the heat pump cycle, the R410a refrigerant is utilized as the working fluid and is defined in Aspen Plus by its composition, which is a mixture of 50% difluoromethane (R-32) and 50% pentafluoroethane (R125) [30]. Also, since the wood pellets are not of unique chemical compound, it is defined in the software as a nonconventional solid component. Later in the process, it is recognized by the solver when decomposed into the conventional compounds of the ultimate analysis (i.e., C, H_2, O_2, N_2, and S) [31]. Furthermore, depending on this analysis, along with the proximate analysis, the properties of nonconventional materials comprising the biomass and ash are defined, where DCOALIGT and HCOALGEN are models that have been used to determine the density and enthalpy, respectively. The different properties of the working fluids in Aspen Plus can be determined based on the selected property method. In this model, a combination of the selected methods, including REFPROP, Peng-Robinson with the Boston-Mathias alpha function (PR-BM), and STEAM-TA, is utilized to estimate the properties of the refrigerant, air and chemical compounds, and water, respectively.

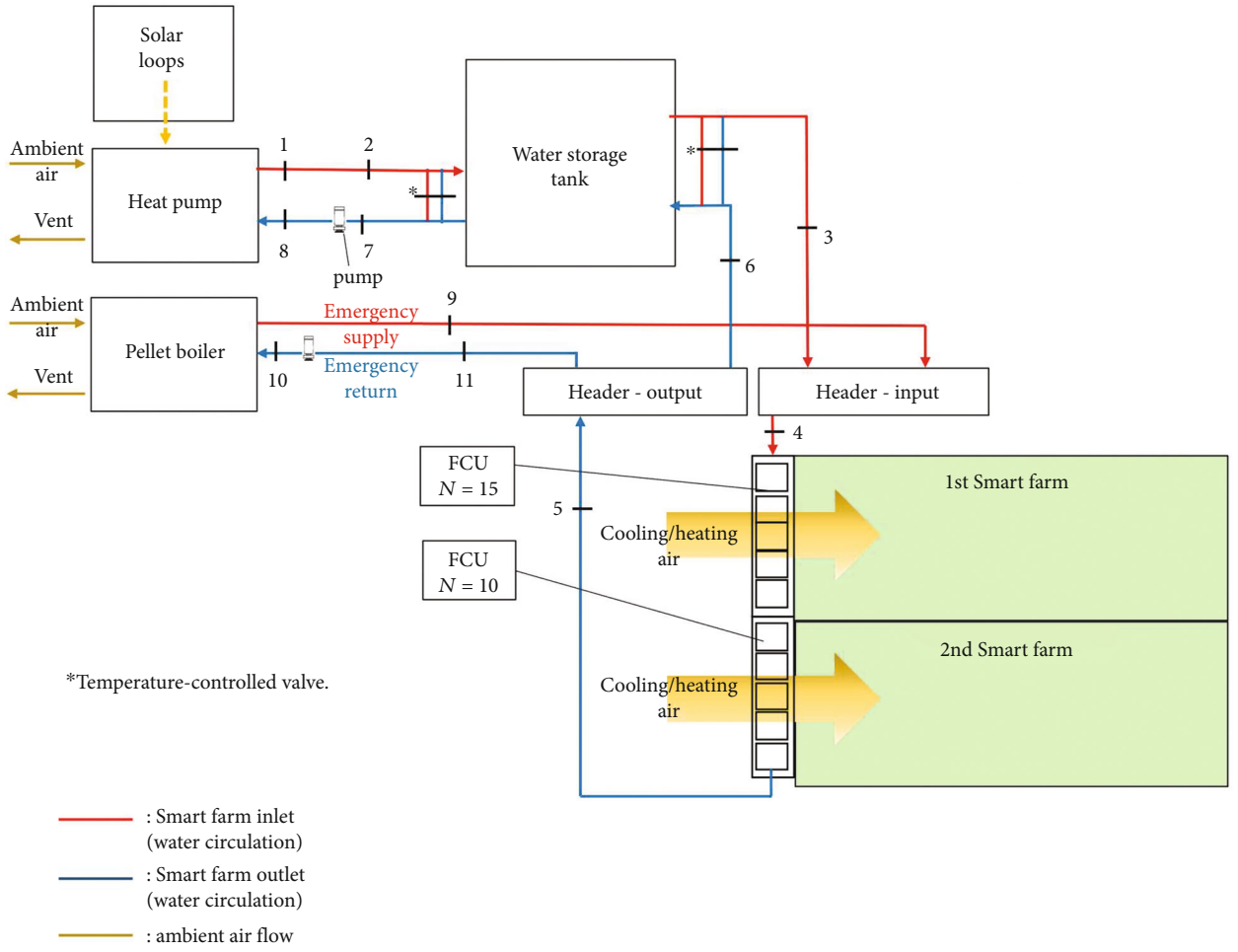

Figure 2: The layout of the smart farm energy system.

Figure 3 shows the process flow diagram of the energy system during the winter mode, which consists of the heat pump, the storage tank, the wood pellet boiler, and the FCUs. In this system configuration, the air-source heat pump works on the vapor compression cycle, and it is utilized to heat the water that is circulated to the storage tank. The refrigerant of the heat pump is compressed in the compressor with a pressure ratio of 3.5, where the expansion pressure is 6.5 bar, and this is within the typical operation ranges of the refrigeration cycle [32, 33]. In addition, the isentropic and mechanical efficiencies of the compression work are 75% and 95%, respectively. The specifications of the evaporator and condenser heat exchangers are a vapor fraction of 1 and a subcooling with 3 degrees, respectively. Accordingly, the heat pump cycle with respect to the saturation lines of the refrigerant is plotted on the P-h diagram as shown in Figure 4. For the summer mode, another Aspen file is created in which the two heat exchangers of the heat pump are exchanged, such that the circulating water of the storage tank is connected to the evaporator instead of the condenser.

The sizing of the system is based on the total cooling capacity of the heat pumps as mentioned in Table 1, which is 325 kW_{th} for the evaporator, and therefore, the flow rate of the refrigerant is determined to be 7250 kg/h. Based on this capacity and with the assistance of the utility tool in Aspen Plus, the corresponding flow rates of the air over the evaporator and the water through the condenser are 44.44 kg/s and 5.5 kg/s, respectively. The water is implemented to extract heat from the condenser of the heat pump in winter and to reject the heat to the evaporator in the summer mode. Here, a thermal storage tank has been incorporated into the design to store the energy of the heated or the cooled water, and it is modelled as a crossflow heat exchanger. The heat exchanger is pinched to 5°C at the cold side. This storage tank, in return, heats up or cools down another water stream that circulates to the FCUs in the winter and summer, respectively.

The COP of the heat pump is evaluated as the ratio between the amount of heat transferred to the water in the condenser (wintertime) or from the water in the evaporator (summertime) $\dot{Q}_{water}$ (W) and the compressor power $\dot{W}_{comp}$ (W), namely,

$$\mathrm{COP}_{HP} = \frac{\dot{Q}_{water}}{\dot{W}_{comp}}. \tag{3}$$

This compressor work is provided by the solar PV array in both the cases of heating and cooling; however, this energy source is not available all day, and this is where the

Table 1: Specifications of the implemented heat pump and boiler.

Heat pump specifications	
Number of units	5
Evaporator capacity (each)	65 kW
Cooling power consumption (each)	20.3 kW
Heating power consumption (each)	21.5 kW
Isentropic efficiency	0.7
Mechanical efficiency	0.9
Refrigerant	R410a
Minimum temperature	-6°C
Maximum temperature	77°C
Ref. mass flow rate (each)	0.4 kg/s
Water flow rate—cooling (each)	3.1 kg/s
Water flow rate—heating (each)	3.33 kg/s
Air flow rate (condenser-summer) (each)	8.05 kg/s
Expansion valve pressure	6.5 bar
Biomass boiler specifications	
Fuel	Wood pellets
Capacity (kW)	456 kW
Fuel consumption	106.5 kg/h
Heat efficiency	82.5%
Water volume of tube	630 L
Fuel LHV	17.37 MJ/kg

Table 2: Specifications of the utilized PV array [29].

Rated power (W)	665
Module efficiency (%)	21.4%
Operating current (A)	17.28 A
Operating voltage (V)	38.5 V
Open circuit voltage (V)	45.6 V
Short circuit current (A)	18.51 A
NOCT	42°C
Temperature coefficient (α)	-0.26%/°C
Lifetime	20 y
No. of modules	600

role of the wood pellet-fired boiler augments the reliability of the system. Furthermore, the boiler is also ready to engage into the system when the ambient air temperature is too low during the wintertime. The wood pellet boiler is simulated firstly as a complete combustion of the pellets by following the equilibrium modelling approach. Secondly, the hot flue gas from the combustor is to be directed to a heat exchanger to boil the water for heating. It is worth noting that the wood pellet is defined as a nonconventional component and, therefore, its heat of combustion is to be defined in Aspen Plus as a pure component parameter. The heating value and the ultimate and proximate analyses, as received from a local supplier in the farm, are reported in Table 3.

The simulation procedure of the biomass combustion starts with the decomposition of the biomass in a RYield reactor (DECOMP) to its conventional components, i.e., carbon, H_2, N_2, O_2, S, and H_2O, in addition to the ash fraction. This yield is worked out through a Fortran calculator to preserve the mass balance between the biomass and the yielded components. The ash content is to be separated from the main material stream before the combustor, where the combustion reactions take place following the equilibrium approach in the modelling. This equilibrium condition is achieved by attaining the minimum Gibbs free energy in the RGibbs reactor (BURN), where the combustible components along with the air are introduced. The amount of air that is required to completely burn the fuel is estimated based on the stoichiometric air to fuel mass ratio $(A/f)_{\text{stoich}}$ which can be calculated as follows [34]:

$$\left(\frac{A}{f}\right)_{\text{stoich}} = \frac{1.293}{0.21}\left(1.866\frac{C}{100} + 5.55\frac{H}{100} + 0.7\frac{H}{100} - 0.7\frac{O}{100}\right), \quad (4)$$

where the values of C, H, S, and O are the dry ash-free mass fractions of the biomass and can be obtained from the ultimate analysis in Table 3. It is considered that the air is introduced with an excess ratio of 1.8, which is within the applicable range of boilers [35, 36], and it is calculated in a calculator block (AFR-BURN). Thus, the mass flow rate of the air, in accordance with the mass flow rate of the wood pellets, is estimated and applied to the air stream flow. For the heat integration between the decomposition and combustion of biomass, a heat stream (Q-DECOMP) is connected between the RYield reactor (DECOMP) and the RGibbs reactor (BURN). The heating capacity of the boiler is 454 kW with an efficiency of 82.5%, and the wood feeding rate is 106.5 kg/h. The flue gas is sent to a common separator to remove the ash stream, and then, it is directed to the boiler heat exchanger (BOILER). The specification of this heat exchanger is that the exit temperature of the flue gas is 150°C and hence the boiling water is fed by a flow rate of 0.1416 kg/s to produce saturated water vapor.

It is important to point out that the storage tank is set up to serve the heat pumps and hence it is connected to the water circuit that exchanges the heat with the heat pump as can be seen in Figure 3. Since the heat pump is the main component for the cooling and heating operation, the storage tank is not connected to the wood pellet boiler, which operates with a stable and consistent performance, and it is less dependent on the ambient condition. The storage tank is modelled in Aspen as a crossflow heat exchanger, where its specification is set to "Hot outlet cold inlet temperature difference = 5 °C" for the winter mode and "Hot inlet cold outlet temp. difference = 5 °C" for the summer mode. In the smart farm energy system configuration, the water from the storage tank or the boiler is provided to the FCUs, which have been incorporated into the design to perform the sensible heating or cooling of the air that is circulated for conditioning the farm. Two main Aspen Plus blocks have been utilized to model this air-conditioning system, namely, a fan block (FANS) with a multiplier block as the design is to include 25 fan units and a heat exchanger (SFARM).

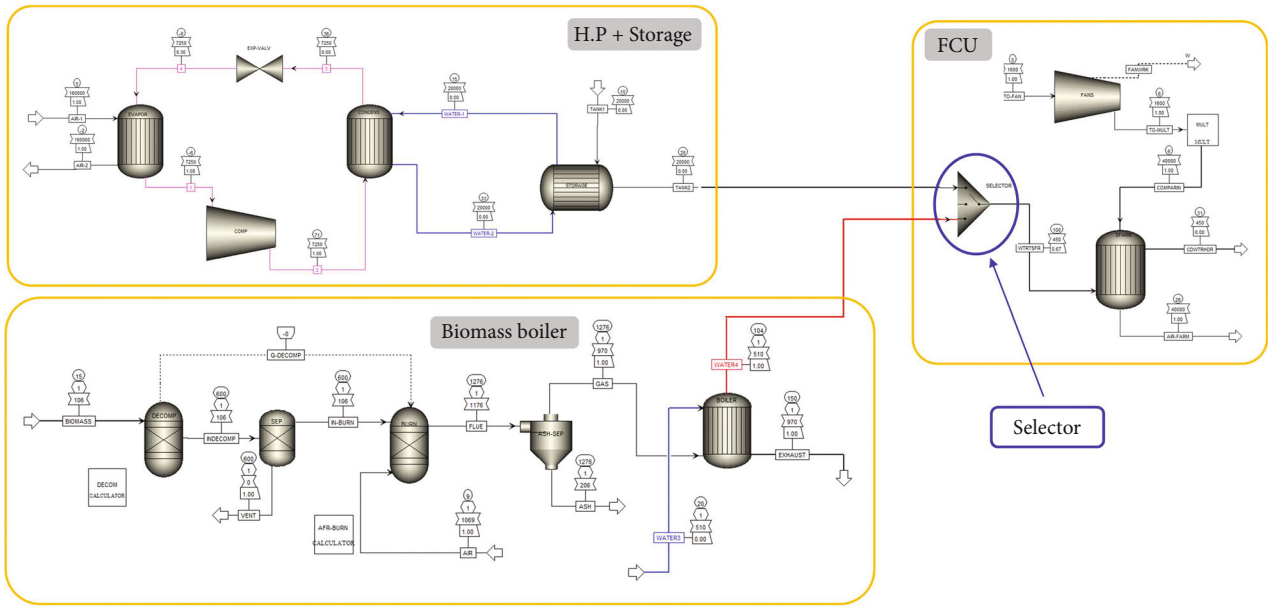

Figure 3: Process flow diagram of the system as implemented in Aspen Plus.

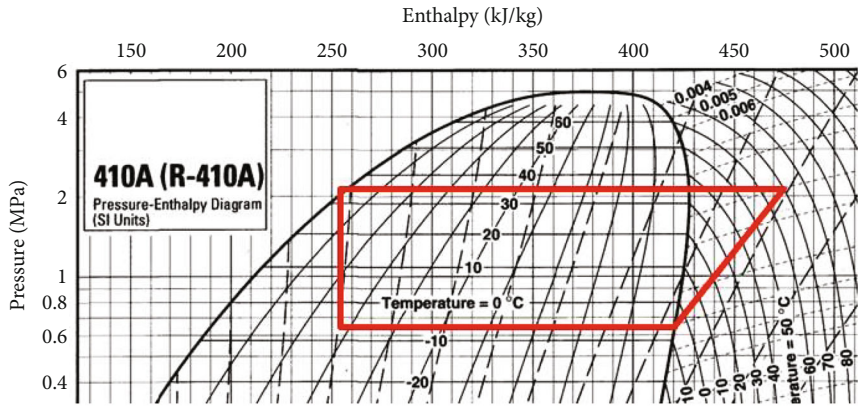

Figure 4: The heat pump cycle on the P-h diagram.

Table 3: Properties of the wood pellets as received in the farm.

Proximate analysis (wt.% a.r.)				Ultimate analysis (wt.%, dry ash-free basis)					LHV (MJ/kg)
MC	VM	FC	Ash	C	H	N	O	S	17.37
8.10	76.46	15.07	0.37	51.23	6.02	0.11	42.63	0.01	

The fan block draws the ambient air at a flow rate of 0.444 kg/s and blows it over the hot or cold tubes containing the flowing water from the storage tank or the boiler. Given that the temperature of the boiler water is much higher than the storage tank temperature in winter, the specification of the FCUs' heat exchanger has two configurations in order to avoid a simulation error. When the heat pump is the source of hot water, the specification of the heat exchanger is set to "Hot outlet cold inlet temperature difference = 10 °C" and when the boiler is engaged, the specification is changed to "Hot/Cold outlet temperature approach = 5 °C". The control of this conditional specification of the heat exchanger and any control of the variables in the combined system are coded in MATLAB.

The operation of the model starts by importing the weather data, which was collected over the year of 2020 on an hourly basis. The power of the PV array is calculated, and then, MATLAB takes control of running the Aspen files. The control of the switch between the heat pump and the boiler is achieved by MATLAB through the stream selector

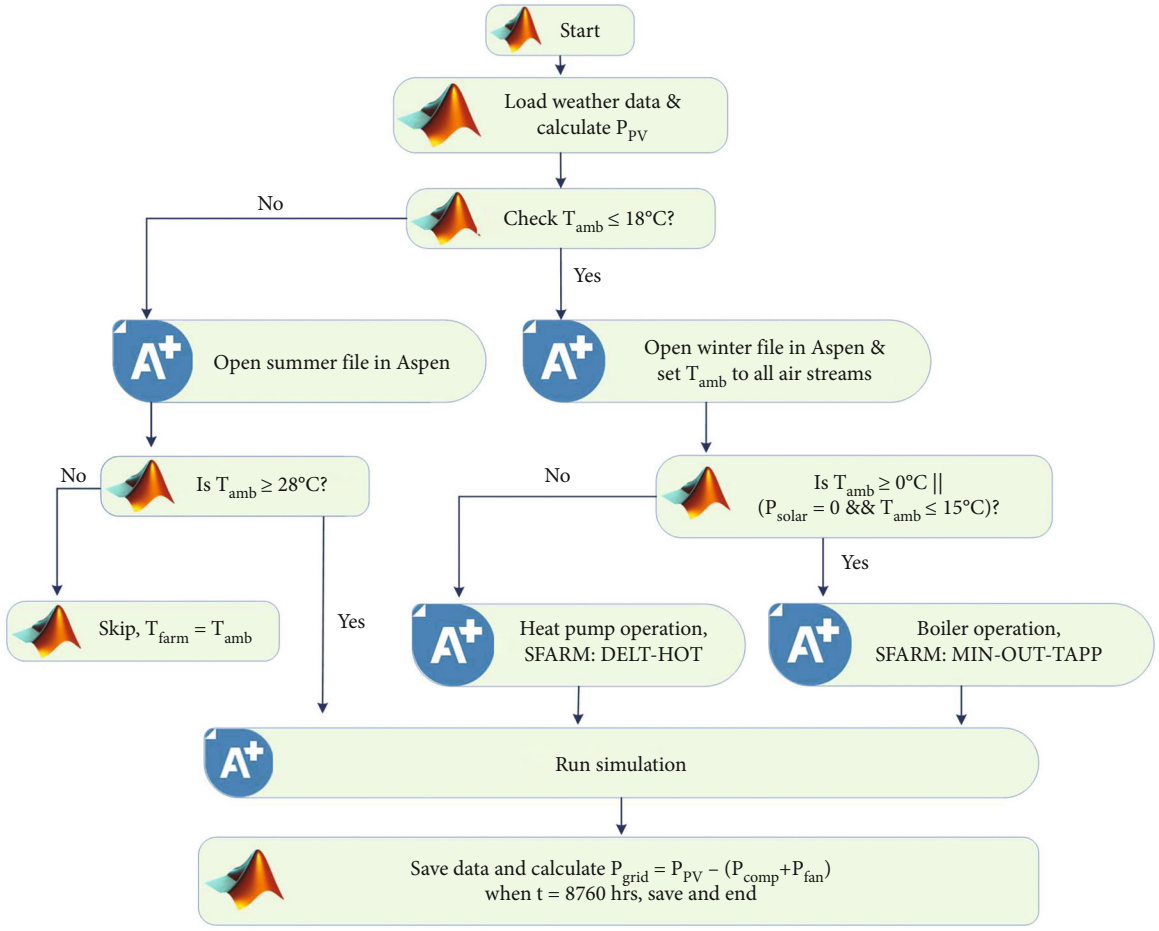

Figure 5: Flow chart of the calculation algorithm.

block "SELECTOR" by connecting the required stream, either the one from the storage tank or the one from the boiler as can be shown in Figure 3. A connection has been established using the MATLAB code to operate and control the Aspen operation through an interchangeable data bridge between the two software platforms using the COM server that is called "actxserver." This server creates an automated object linking and embedding (OLE) on the local system using the program identifier of Aspen Plus, and this is named "Apwn.Document.37.0" [37]. The simulation is carried out for one year on an hourly basis, i.e., a total of 8760 hrs, where MATLAB selects the targeted Aspen file (winter or summer) based on the ambient temperature (T_{amb}).

The calculation algorithm and the interaction between Aspen Plus and MATLAB is illustrated in Figure 5. As shown, the main condition to operate the system in the heating mode (wintertime) is when the ambient temperature is below or equal to 18°C, while the cooling mode is operated when the ambient temperature is above or equal to 28°C. Following this, the corresponding Aspen file is opened, and the ambient temperature is set to all inlet air streams. In the heating mode of the simulation, the selection of the boiler over the heat pump is based on two conditions, namely, when the solar power $(P_{solar}) = 0$ kW or $T_{amb} \leq 0°C$. It is worth mentioning that when any solar energy is available, the grid interacts with the PV array either by covering the shortage of power or receiving the surplus energy produced.

3.2. Economic Analysis. An economic assessment is carried out based on the simulation data, which, in principle, can be achieved by calculating the economic indicators, such as the levelized cost of energy (LCOE), the annualized total cost, or the net present cost of the system. In this study, the LCOE, which is the unit cost of energy supplied to the system over its life cycle, has been deployed as the economic indicator to present the viability of the plant over its entire life. It is the ratio of the net present cost (NPC) of energy to the total energy demand (E) and is calculated as follows [38]:

$$\text{LCOE} = \frac{\text{NPC}}{\sum_{t=1}^{t=8760} E(t)}. \quad (5)$$

The NPC comprises the annualized value of the capital expenditures (ACAPEX) and the annual operation expenditures (OPEX); the latter consists of the maintenance and variable costs. This can be expressed as follows:

$$\text{NPC} = \text{ACAPEX} + \text{OPEX}. \quad (6)$$

Table 4: CAPEX evaluation methodology [41, 42].

Cost component	Factor
Direct cost (DC)	
Purchase cost of equipment (PCE)	
Purchase equipment installation	39% PCE
Instrumentation and control	26% PCE
Piping	31% PCE
Electrical systems	10% PCE
Indirect costs (IDC)	21.9% DC
Fixed capital investment (FCI)	IDC+DC
Start-up costs (SUC)	5% FCI
Total CAPEX	FCI+SUC

CAPEX is the equipment cost with any related installation and acquisition costs, and if distributed over the years of operation under a certain discount rate, the value of ACAPEX would be a one-year fraction of the total CAPEX. However, as the name suggests, NPC considers the ACAPEX after being converted back to the initial time of purchase. Following a discount rate of (i_d) and a project lifetime of (n) years, the ACAPEX can be evaluated by multiplying the capital recovery factor (CRF) to the CAPEX as follows [39, 40]:

$$\text{ACAPEX} = \text{CAPEX} \times \left(\frac{i_d \times (1 + i_d)^n}{-1 + (1 + i_d)^n} \right). \tag{7}$$

For this study, the discount rate and the lifetime are assumed to be 10% and 20 years, respectively. In order to evaluate the capital expenditures (CAPEX), the utilization of a bottom-up technique is followed, in which the cost components are evaluated as fractions of the purchase cost of the equipment (PCE) [41, 42]. This approach considers the direct costs, such as the installation costs, as well as the indirect costs of the system components as shown in Table 4.

The price of a unit with specific size can be estimated in accordance with a reported price for a given unit size in a certain year. To consider the effect of scale on the purchase cost, as well as the price change over time, the scaling exponent correlation and the chemical engineering plant cost index (CEPCI) are utilized, and this can be expressed in the following form [43]:

$$C = C_0 \left(\frac{S}{S_0} \right)^f \times \left(\frac{I_{\text{current}}}{I_{\text{ref}}} \right), \tag{8}$$

where C is the actual current cost of the equipment, C_0 is the unit base cost at the reference year, S and S_0 are the sizes of the actual unit and the reference unit, respectively, and f is an empirically determined exponent. I_{current} and I_{ref} are the corresponding CEPCIs for the current year and the reference year, respectively. For the year of study (2020), I_{recent} is 599.5 whereas I_{ref} depends on the year of the cited cost for each component of the system. The scaling factors for the PV modules, FCUs, and the heat pumps are taken as 1, while for the scaling factors for the storage tank and the boiler, a value of 0.7 is assumed. The implemented cost estimates, represented by the base investment cost along with the corresponding base year for the different components, are outlined in Table 5. For the OPEX, the employed fixed and variable costs of the different equipment are presented in Table 6.

Table 5: Purchase cost of equipment (PCE) for the system components.

Equipment	Base cost	Unit	Base year	f	Reference
Solar PV	1700	\$/kW	2018	1	[44]
Heat pump	332.04	\$/kW$_{\text{th}}$	2016	1	[45]
Thermal storage tank	237.4	\$/m^3	2017	0.7	[46]
Pellet boiler	262.25	\$/kW	2009	0.7	[47]
FCUs	1000	\$/unit	2022	1	[48]

3.3. Environmental Analysis. Another major factor to take into account when introducing a low-carbon energy system is the environmental impact of the hybrid system. This can be achieved by comparing the CO_2 emissions of the system to that of a conventional heating system. Accordingly, the CO_2 emission reduction ratio (CO_2ER) is presented, and it can be evaluated from the following expression [53]:

$$\text{CO}_2\text{ER} = \frac{X^i_{\text{CO}_2} \times Q_{\text{Conv}} - X^Q_{\text{CO}_2} \times Q_{\text{CCHP}} - X^e_{\text{CO}_2} \times E_{\text{CCHP}}}{X^i_{\text{CO}_2} \times Q_{\text{Conv}}}, \tag{9}$$

where $X^i_{\text{CO}_2}$ is the emission factor of the conventional heating system (i) and $X^Q_{\text{CO}_2}$ and $X^e_{\text{CO}_2}$ are the emission factors of the proposed energy system for the heat load, Q_{CCHP}, and for the electricity consumed by the system, E_{CCHP}, respectively. Q_{Conv} is the total heat supply when generated by a conventional system. It should be noted that in our case, the Q_{CCHP} refers only to the boiler heating generation as the heating/cooling produced by the heat pump is incorporated in the energy of the CCHP system (E_{CCHP}).

4. Results and Discussion

4.1. Technical Assessment of the System. Figure 6 depicts the ambient temperature, the solar irradiation, and the corresponding power generated from the PV modules over one year (8760 hours). It can be seen that the temperature fluctuates between -7.5°C (in winter) and as high as 31.5°C (in summer), while the global horizontal irradiation in this location reaches 1018 W/m^2 in the summer months. Accordingly, the PV system generates up to 200 kW during winter, while in the early months of the summer, a peak generation of about 339 kW is achieved.

The system of the PV panels is connected to the grid as a backup source of electricity and as a receiver of surplus

Table 6: OPEX estimation methodology for the system components.

Cost component	Annual fixed O&M	Variable O&M	Unit	Reference
Solar PV	11.3	—	\$/kW	[49]
Heat pump	16.96	0.565	\$/kW$_{th}$ \$/MWh$_{th}$	[49]
Thermal storage tank	3% of the component PCE	—		[50]
Pellet boiler	5% of the component PCE	37.3	\$/MWh	[51]
Wood pellets	—	74	\$/tonne	[51]
Surplus electricity	—	0.098	\$/kWh	[52]

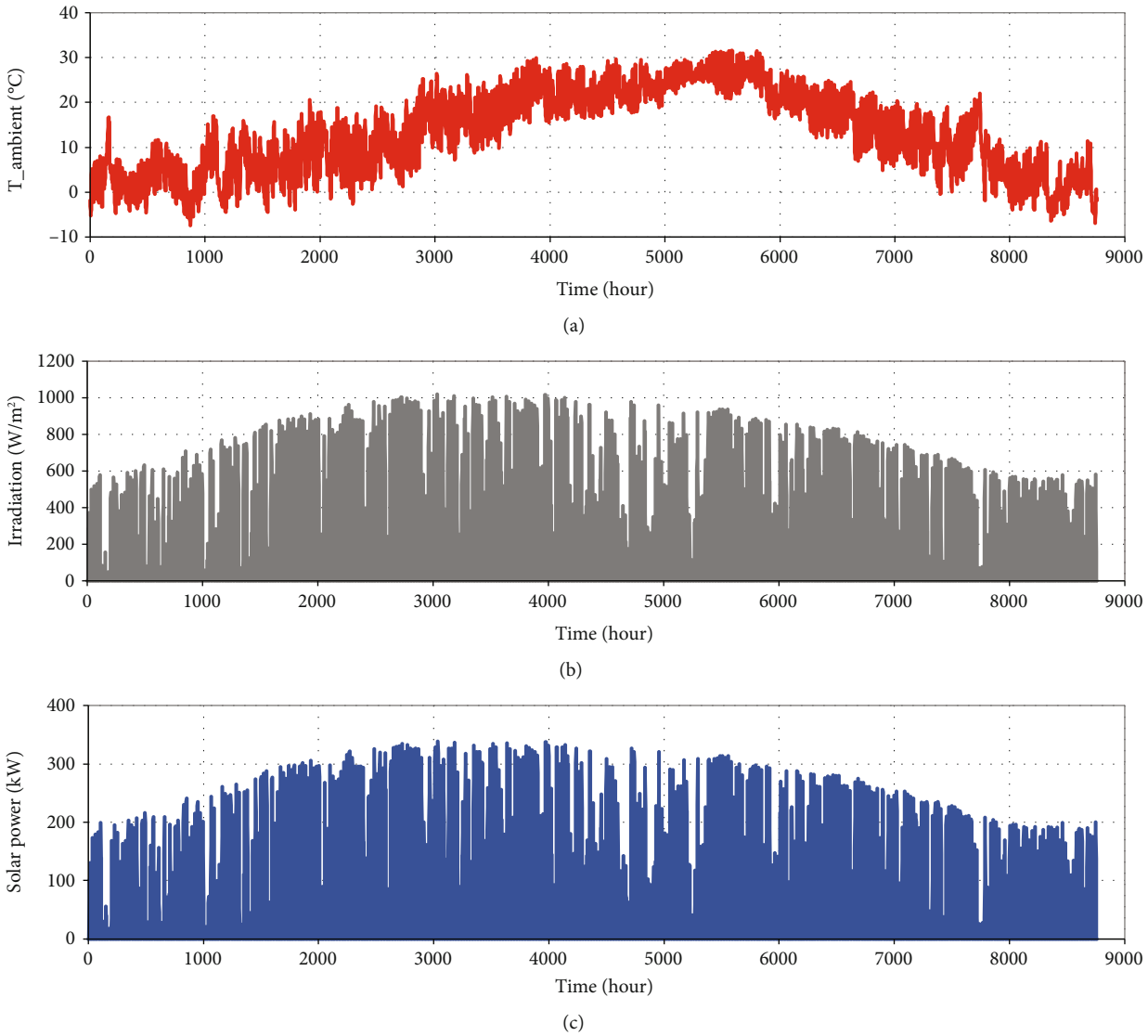

Figure 6: The ambient temperature (a), the solar irradiation (b), and the PV power generation (c) across one year at the smart farm location.

power. The simulation results of the system show the power consumption and how much electricity is being exchanged between the PV panels and the grid, and this is exhibited in Figure 7. Most of the electricity that is received from the grid is in the low temperature period of time, while in most of the summertime, the electricity from the PV panels is exported to the grid. The total annual electricity consumption by the farm is 367.16 MWh. The solar panels provide 234.12 MWh in real-time operation while the remaining 133.04 MWh is covered by the grid. However, when considering the annual accumulated electricity generation from PV arrays, the system exports 332.62 MWh to the grid, and hence, the energy system is a net exporter of electricity with 199.58 MWh.

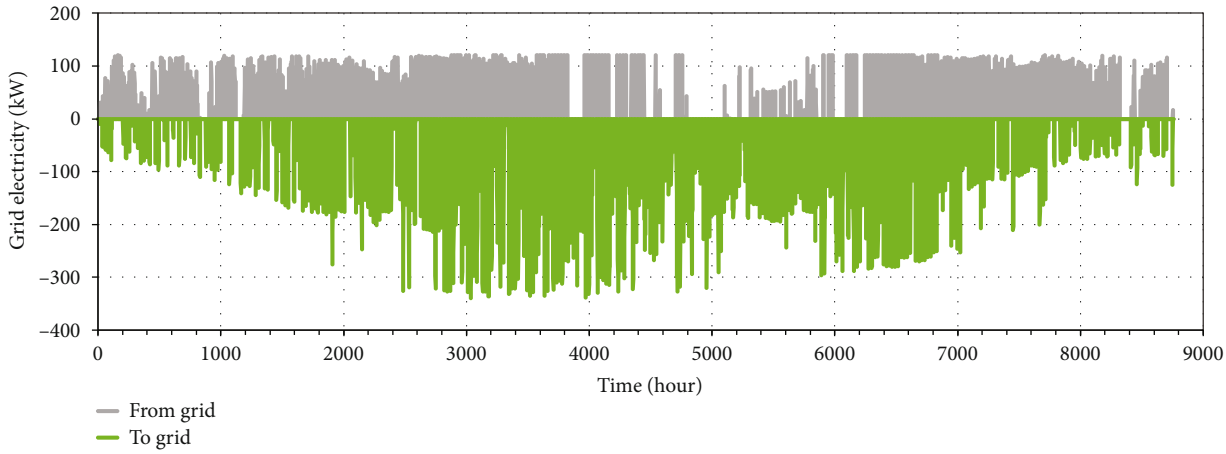

Figure 7: Power exchange between the PV array and the grid over one year.

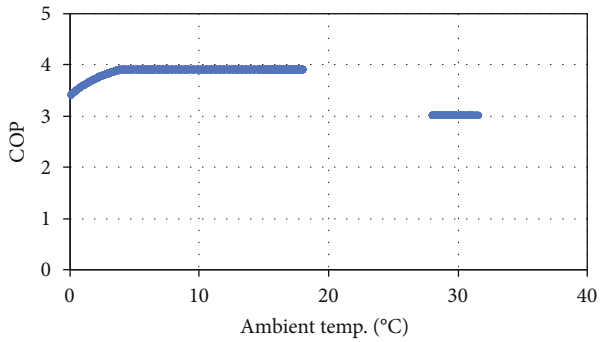

Figure 8: The COP of the heat pump for different ambient temperatures.

The generated power from the solar arrays, backed by the grid, is directed to run the heat pump as the primary option to meet the demand of the smart farm. The COP of the heat pump is estimated at about 4 for the heating mode and at about 3 for the cooling mode as shown in Figure 8. The heat pump is running at a constant COP value in both the heating and cooling modes, and this is because of the assumed fixed pressure ratio and the fixed design specifications of the two heat exchangers (evaporator and condenser) as discussed in Section 3.1. Nevertheless, Figure 8 shows that in winter, at the relatively intense cold temperatures (<4°C), the COP expectedly drops down to approximately 3.4 as there is not enough heat available from the air to achieve the design specification of the evaporator, i.e., the refrigerant vapor fraction = 1. When the ambient temperature is between 18°C and 28°C, the heat pump is shut down, and hence, no relevant COP values are presented in Figure 8. The average COP over one year, also known as the seasonal performance factor, is calculated as 3.85.

The predicted average temperature and the average heat load of the farm over one year on a daily basis are shown in Figure 9. It can be seen in Figure 9(a) that the temperature is, in the vast majority of the cases, above 20°C and mostly fluctuates around 24°C and these conditions are satisfactory for the farm operation [18]. In Figure 9(b), the average farm heat load is at the highest value in the winter period at about 220 kW when the ambient temperature is low, and this load decreases as it moves towards the summer period. Also, it is noticeable that for about 100 days (from about the 160th day to about the 260th day), the heat load is negligible, and this is because the ambient temperature is in the targeted range of the operating temperature. In the summer, the cooling load of the farm has been satisfied by the heat pump for limited operational days, which are represented by the red dots in Figure 9(b).

4.2. Economic Evaluation. Based on the operating conditions and the simulation data, the economic evaluation of the energy system has been carried out. Figure 10 shows how the CAPEX is broken down between the different components of the system. It can be seen that the PV panels and the biomass boiler share most of the CAPEX with about 80% and with almost equal share of this amount. In addition, the heat pump is responsible for 16%, and the balance is attributed to the FCUs and the thermal storage tank. From a CAPEX perspective, the PV-heat pump combination is more expensive than the biomass boiler as modes of operation for heating. Nevertheless, the purchase cost of the equipment (PCE) or CAPEX cannot be the one and only economic criterion of any system, but rather, the OPEX is of the same vitality as an economic evaluating parameter.

As depicted in Figure 11, the fixed and variable costs of the biomass boiler (i.e., the operation and maintenance cost and the wood pellet cost, respectively) are responsible for the majority of the expenditures by a high margin, i.e., about 68% of the total OPEX, whereas the share of both the heat pump and the PV panels is only 25%, and hence, this combination is less OPEX-intensive than the boiler. The rest of the OPEX is 6% for the FCUs and 1% for the thermal storage tank.

The total annual energy demand by the farm is 1075.87 MWh_{th}, which is utilized to estimate the ACAPEX and OPEX of the energy system. Accordingly, the LCOE has been estimated by using equation (5) at $0.218/kWh. The estimated LCOE lies within the range of the reported energy costs ($0.14-0.287/kWh) for greenhouses coupled to

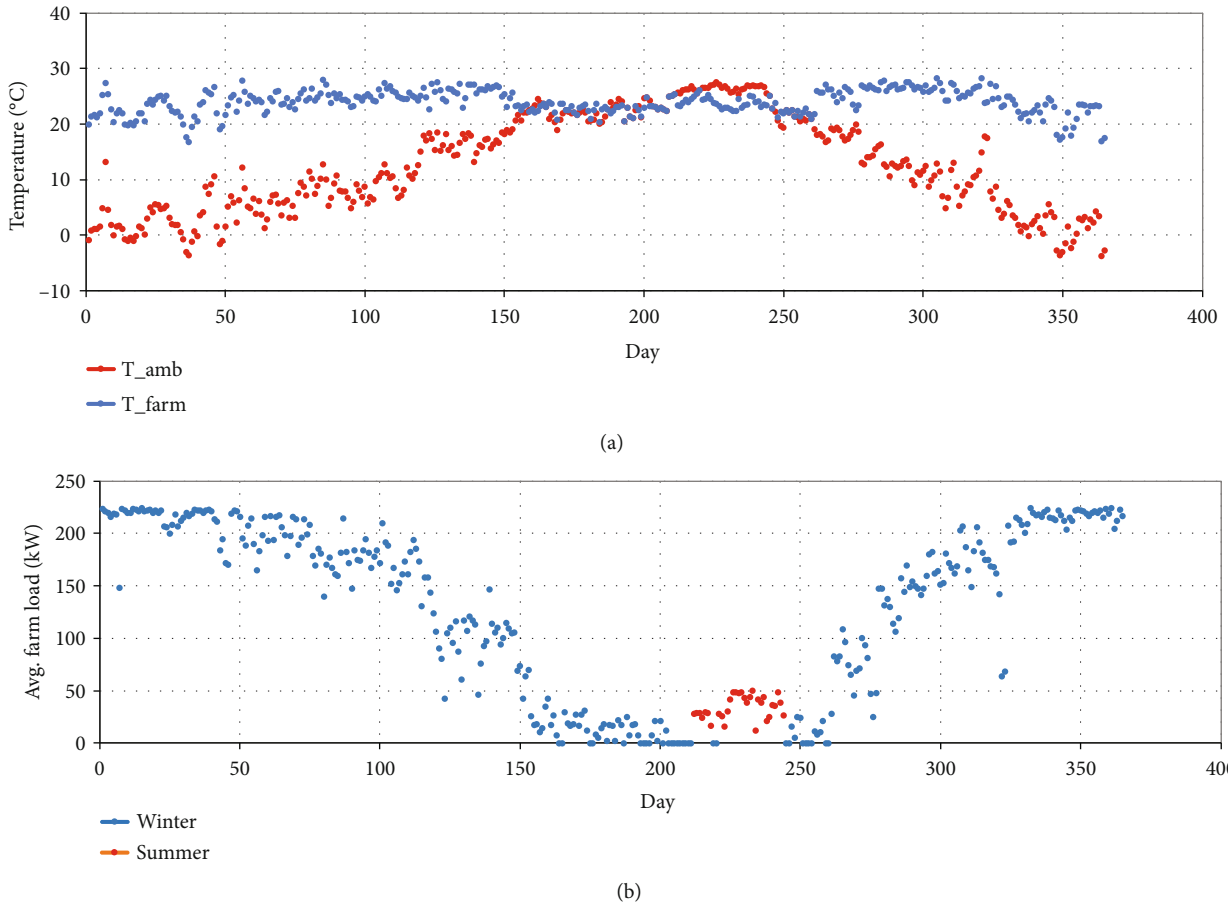

Figure 9: The predicted farm temperature (a) and the average farm heat load (b) on a daily basis over one year; red dots in graph (b) refer to cooling load.

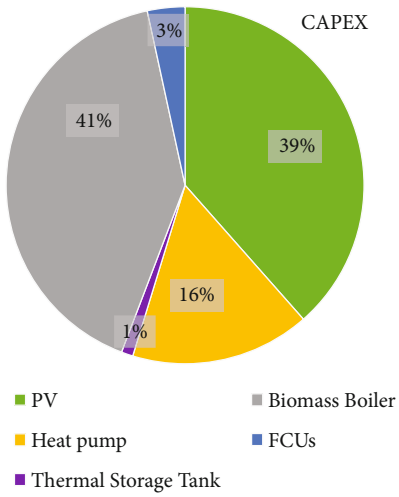

Figure 10: Breakdown of the CAPEX between the system components.

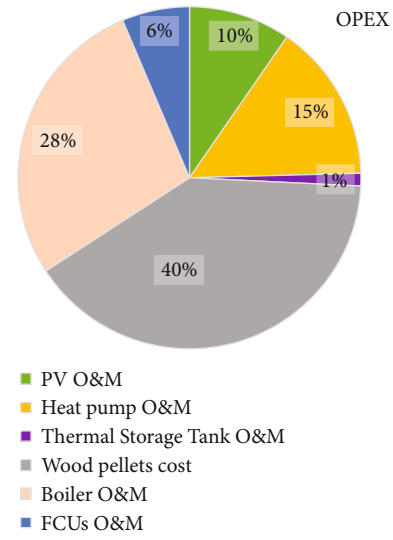

Figure 11: Breakdown of the OPEX between the system components.

geothermal heat pumps in the IPCC report "Summary for Policymakers of 2012" [54, 55]. For comparison purposes, a grid-connected GSHP system in China for greenhouse heating has an estimated LCOE of $0.4/kWh [13].

Further, Figure 12 depicts that the energy system is CAPEX-intensive over the OPEX and the boiler system (due to the biomass cost) is the major cost contributor to

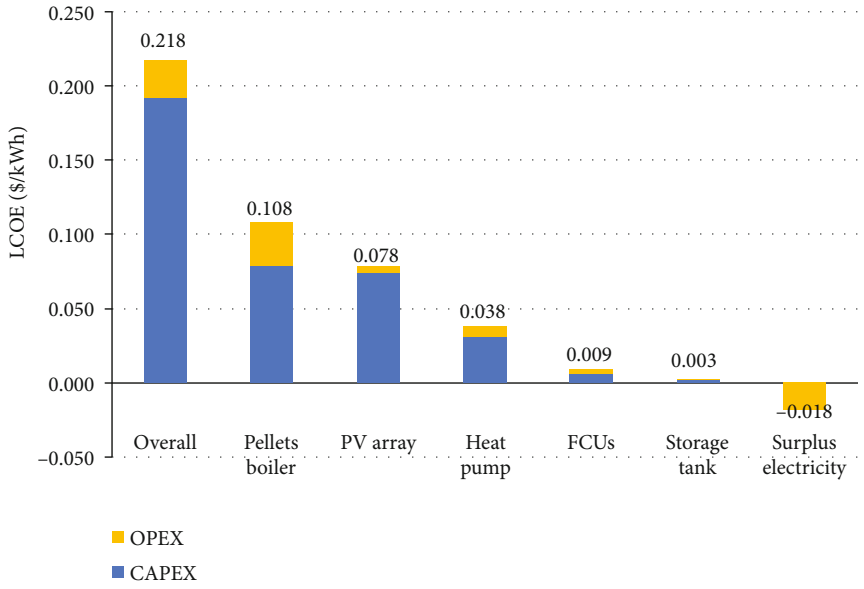

Figure 12: The LCOE breakdown.

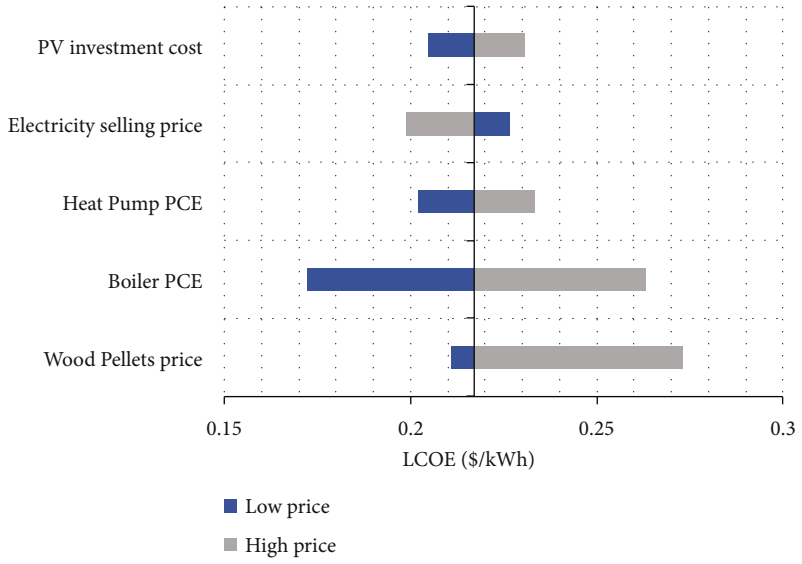

Figure 13: Sensitivity of the LCOE on the different cost parameters.

the OPEX as the PV followed by the heat pump do not need major operation and maintenance costs. Also, it can be seen that the surplus electricity from the PV arrays over one year (199.58 MWh) can reduce the LCOE by $0.018/kWh. This represents a reduction by 23.1% of the net annual contribution by the PV system (i.e., $0.078/kWh).

4.3. Sensitivity Analysis. The calculation of the LCOE is based on the applied cost for the different system components, but this cost may have a considerable margin of uncertainty. Hence, a sensitivity analysis can give a good indication on the contribution of each factor into the LCOE. Figure 13 illustrates the share of the most important cost components that would affect the LCOE, such as the purchase prices of the PV panels, the heat pump, and the boiler. The adopted cost for the PV corresponds to commercial/industrial scale (i.e., $1700/kW); we have assumed as lower bound for this cost the utility-scale PV cost in Korea, i.e., $1300/kW [44]. A similar increase by $300/kW is assumed as the possible higher price. For the heat pump and the boiler PCE, a variation of ±50% is considered. Also, two main variable costs are considered: the biomass price and the electricity selling price. A wide range has been considered for the feedstock cost to capture the relatively high uncertainty of wood pellet cost. Similarly, a wide range of values is considered for the electricity costs. The boundaries of change for each investigated cost component are shown in Table 7.

Table 7: Proposed boundaries of change for the sensitivity analysis.

Parameter	Lower price	Nominal price	Higher price	Unit
PV investment cost	1400	1700	2000	\$/kW
Electricity selling price	0.05	0.098	0.2	\$/kWh
Heat pump PCE	166	332.04	498	\$/kW
Boiler PCE	655.6	1311.3	1967	k\$/5MW$_{th}$
Biomass price	50	74	310	\$/tonne

Table 8: The emission factors for different heating sources and the corresponding emission reduction.

Emission factors	Smart farm	Electricity (Korean grid)	NG boiler	Oil boiler	Gas boiler	LPG boiler	Wood chip boiler	Wood pellet boiler
kgCO_2-eq/kWh [56, 57]	0.056 (calculated)	0.666	0.22	0.27	0.235	0.273	0.0312	0.0244
CO_2ER (%)	—	85.42	86.28	88.82	87.15	88.94	3.36	-23.9*

*The minus symbol means that the proposed system emits more than the conventional.

As shown in Figure 13 and due to the relatively high boiler purchase cost, the change in its price leads to a noticeable variation in the LCOE of around ±20.8%. The variation in the investment cost of the PV panels and the heat pump results in the LCOE to vary within ±6% and ±7.2%, respectively. Further, it can be observed that the LCOE is highly sensitive to biomass cost, and for the extreme case of \$310/tonne of wood pellets, the LCOE increases to \$0.273/kWh (an increase of 25.2%). Hence, the establishment of a long-standing biomass procurement deal with determined quantities and charges should be chased with an agricultural or forest management company. This highlights the importance of establishing the long-term supply of biomass at a fixed price. In addition, the electricity selling price to the grid can contribute to the reduction of the energy price down to \$0.2/kWh, and this can be achieved as the electricity exported may be eligible to receive renewable energy tariffs. It can be noticed that the LCOE is more sensitive to the boiler costs, and hence, the combination of the PV panels with the heat pump should have the priority over the boiler to operate when the solar energy is available.

4.4. Carbon Footprint. In order to study the carbon footprint of the smart farm energy system in comparison to other conventional systems, the emission factors for the different heating technologies are tabulated in Table 8. The emission factors of the PV array (0.0826 kgCO_2-eq/kWh) and the grid electricity in Korea (0.666 kgCO_2-eq/kWh) are taken from the SimaPro software, while for the boilers, the emission factors have been taken from relevant literatures. In this study, it is assumed that the conventional electric-based heating is to run a heat pump with the same COP as that of the smart farm's heat pump in order to satisfy the total energy demand of the farm. Also, as discussed in Section 4.1, the majority of the energy demand is for heating, and therefore, the other conventional energy systems are different types of boilers with the cooling load neglected. This means that the proposed new energy system can achieve even higher CO_2 reductions, and this is very important. The calculated emission factor of the proposed system is 0.056 kgCO_2-eq/kWh. This is much less than the hybrid system that has been investigated for another Korean smart farm with a wood pellet boiler and a grid electricity-based hydrothermal heat pump, i.e., 0.424 kgCO_2-eq/kWh [24]. This highlights the sustainability gains of our proposed design and the necessity to design systems with low reliance on the grid. Also, it can be seen that the proposed smart farm can achieve a significant emission reduction of between 85.42% and 88.94% when replacing a grid-connected heat pump or fossil fuel-based heating boilers. The achieved emission reduction is higher than the value that has been reported by Zhou et al. [14], which was 35.5%. This value was attained when using a GSHP connected with a fuel oil heater in a hybrid system as a compared to the oil heater only. This shows the significant environmental benefits of employing the pellet boiler and the solar PV panels, as in the current study.

Compared to the wood chip boiler, the hybrid energy system has higher emission factor; however, the smart farm still reports a small CO_2ER because of the heat pump COP being high enough (seasonal performance factor of 3.85). This implies that the overall amount of energy needed, to achieve the same heating load, is less than the boiler. However, when compared to the wood pellet boiler, the smart farm emits more CO_2. It should be noted that the greenhouse energy system is a net exporter of electricity, and this has not been considered in the current carbon footprint analysis. Therefore, the net emission of the smart farm could have been reduced even further if we were to consider that the green-exported electricity displaces grid electricity.

Figure 14 illustrates the amount of the CO_2 emission that is being released from the smart farm in comparison to the fossil fuel-based heating, biomass-based heating, and electricity-based heating. The smart farm emits only 60.2 tCO_2/y, while the emissions from the fossil fuel-based heating systems can go up to 544.5 tCO_2/y. In comparison to the biomass-based heating boilers, the green energy system is still comparable, and even the smart farm energy system runs more hours for cooling. Since the smart farm energy system is a combination of a wood pellet boiler and PV panels, the carbon footprint of the smart farm is slightly

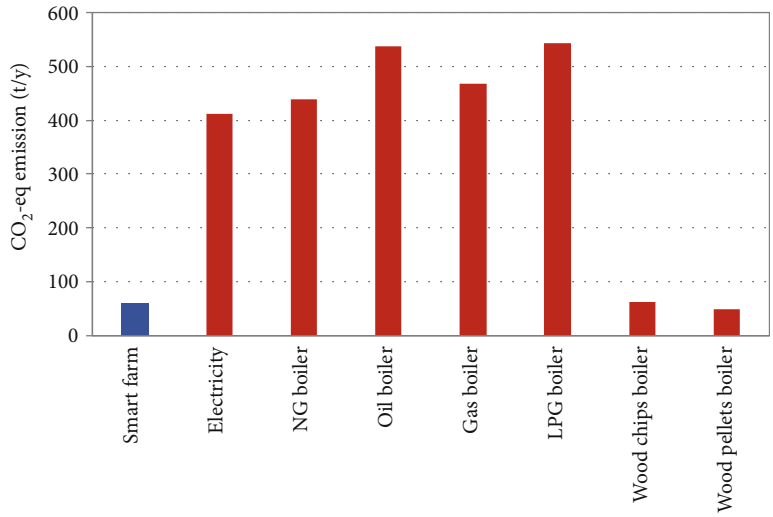

Figure 14: Quantitative comparison of the CO_2 emission between the green system and other separate heating systems.

higher than the single wood pellet boiler by 11.62 tCO_2/y. This is because of the relatively higher emission factor of the PV array.

5. Conclusion

This study presents a techno-enviroeconomic investigation of a decentralized renewable CCHP system for a smart farm located in South Korea. This energy system comprises solar PV panels, ASHP, and a wood pellet boiler in a hybrid configuration for greenhouse farm application. A novel dynamic modelling approach has been developed and applied to simulate the operation of the energy system on an hourly basis. The model implements an interchangeable operation of the PV-heat pump and the wood pellet boiler. The major and important outcomes of this study are as follows:

(i) The synchronized operation of the hybrid energy system model has provided reliable dynamic operation to maintain the energy demand of the farm with any surplus electricity being exported to the grid

(ii) Technically, the hybrid energy system has achieved an average daily temperature in the farm around 23.9°C and fluctuates with a standard deviation value of 2.16°C, while the seasonal performance factor of the heat pump is estimated at 3.85 over one year

(iii) By utilizing the technical thermodynamic data, the LCOE is estimated at $0.218/kWh, and the total annual energy demand of the farm is 1075.87 MWh_{th}. This implies that the system without subsidies cannot compete with conventional energy systems

(iv) The priority for prime energy is given to the PV-heat pump combination over the wood pellet boiler due to the higher energy efficiencies

(v) For the given economic assumptions, as the energy dependency moves from the PV to the boiler, the higher the cost of energy becomes, and this is attributed to the high running costs of the boiler

(vi) It is worth noting that the PV panels help in reducing the LCOE by $0.018/kWh through exporting the surplus electricity to the grid over the year

(vii) From an environmental perspective, the carbon footprint of the greenhouse energy system is significantly lower than the conventional heating systems, such that the achieved CO_2ER varies between 85.42% and 88.94% when compared to the electric-based or fossil fuel-based heating systems

(viii) The quantity of CO_2 that could be emitted by the greenhouse energy system is 60.2 tCO_2/y, which is equivalent to an emission factor of 0.056 $kgCO_2$-eq/kWh

The current study presents reliable design and assessments that can provide meaningful insights for the transition of the farming sector to renewable decentralized energy solutions. The resilience of such hybrid energy systems can be increased by including waste to energy technologies, such as gasification and biomethanation along with different energy storage technologies.

Symbols

a: Ambient
Ann: Annualized
a.r.: As received
avg: Average
c: Cell
CCHP: Combined cooling, heating, and power
CHP: Combined heat and power
d: Discount

diss: Dissipation
d.a.f: Dry ash free
e: Electricity
ER: Equivalence ratio
FCUs: Fan coil units
FC: Fixed carbon
gen: Generation
GHG: Greenhouse gas
Q: Heat
LPG: Liquefied petroleum gas
l: Load
LHV: Lower heating value
RGibbs: Minimum Gibbs free energy reactor
MC: Moisture content
NPC: Net present cost
NOCT: Normal operating cell temperature
OLE: Object linking and embedding
O&M: Operation and maintenance
PV: Photovoltaic
PCE: Purchase cost of equipment
ref: Reference
STC: Standard test condition
stoich: Stoichiometric
VM: Volatile matter
wt.%: Weight percent
C: Cost ($)
F: Power loss (W)
G: Solar irradiance (W/m^2)
$\dot{m}$: Mass flow rate (kg/h)
n: Component life (year)
P: Power (W)
T: Temperature (K)
T_o: Reference temperature (K)
V: Voltage (V)
α: Temperature coefficient (%/°C)
X: Emission factor ($kgCO_2/kWh$)
I: Scale index (-).

Data Availability

Modelling data will be available upon request.

Conflicts of Interest

The authors declare that there is no conflict of interest that could be perceived to affect the objectivity or neutrality of the manuscript.

Acknowledgments

This study has been conducted with the support of the Korea Institute of Industrial Technology as part of the project "Development of a design tool for a smart farm energy system integrated with renewable energies optimized to economics, environment and low-carbon emission (2/2)" (KITECH JE-22-0002).

Supplementary Materials

The supplementary material holds the relevant weather data that were obtained from the weather station in the city of Naju, Republic of Korea. The coordinates of the smart farm are 35°1′29.28″N and 126°49′42.6″E. *(Supplementary Materials)*

References

[1] S. Pellegrino, A. Lanzini, and P. Leone, "Techno-economic and policy requirements for the market-entry of the fuel cell micro-CHP system in the residential sector," *Applied Energy*, vol. 143, pp. 370–382, 2015.

[2] L. Kitzing, C. Mitchell, and P. E. Morthorst, "Renewable energy policies in Europe: converging or diverging?," *Energy Policy*, vol. 51, pp. 192–201, 2012.

[3] A. Piacentino, C. Barbaro, F. Cardona, R. Gallea, and E. Cardona, "A comprehensive tool for efficient design and operation of polygeneration-based energy μgrids serving a cluster of buildings. Part I: description of the method," *Applied Energy*, vol. 111, pp. 1204–1221, 2013.

[4] M. Renzi and C. Brandoni, "Study and application of a regenerative Stirling cogeneration device based on biomass combustion," *Applied Thermal Engineering*, vol. 67, no. 1-2, pp. 341–351, 2014.

[5] *Government to Promote 5G Services and Fintech*, Ministry of Economy and Finance, 2019, https://www.moef.go.kr/nw/nes/detailNesDtaView.do?menuNo=4010100&searchNttId1=MOSF_000000000026977&searchBbsId1=MOSFBBS_000000000028.

[6] C.-G. Lee, L.-H. Cho, S.-J. Kim, S.-Y. Park, and D.-H. Kim, "Prediction model for the internal temperature of a greenhouse with a water-to-water heat pump using a pellet boiler as a heat source using building energy simulation," *Energies*, vol. 15, no. 15, p. 5677, 2022.

[7] C.-G. Lee, L.-H. Cho, S.-J. Kim, S.-Y. Park, and D.-H. Kim, "Comparative analysis of combined heating systems involving the use of renewable energy for greenhouse heating," *Energies*, vol. 14, no. 20, p. 6603, 2021.

[8] Government of the Republic of Korea, *2050 Carbon Neutral Strategy of the Republic of Korea: towards a Sustainable and Green Society*, The Government of the Republic of Korea Seoul, Seoul, Korea, 2020.

[9] H. Sithole, T. Cockerill, K. Hughes et al., "Developing an optimal electricity generation mix for the UK 2050 future," *Energy*, vol. 100, pp. 363–373, 2016.

[10] S. Gorjian, R. Singh, A. Shukla, and A. R. Mazhar, "On-farm applications of solar PV systems," in *Photovoltaic Solar Energy Conversion*, pp. 147–190, Elsevier, 2020.

[11] H. Benli, "A performance comparison between a horizontal source and a vertical source heat pump systems for a greenhouse heating in the mild climate Elaziğ, Turkey," *Applied Thermal Engineering*, vol. 50, no. 1, pp. 197–206, 2013.

[12] L. Chai, C. Ma, and J.-Q. Ni, "Performance evaluation of ground source heat pump system for greenhouse heating in northern China," *Biosystems Engineering*, vol. 111, no. 1, pp. 107–117, 2012.

[13] J. Luo, W. Xue, and H. Shao, "Thermo-economic comparison of coal-fired boiler-based and groundwater-heat-pump based heating and cooling solution–a case study on a greenhouse in

Hubei, China," *Energy and Buildings*, vol. 223, article 110214, 2020.

[14] M. Zhou, F. Cai, M. Uenishi, and Y. Sekine, "Performance evaluation of a hybrid heating system combined a groundwater source heat pump with an existing fuel oil heater for a horticultural greenhouse," *International Journal of Green Energy*, vol. 19, no. 13, pp. 1404–1414, 2022.

[15] S. Awani, R. Chargui, S. Kooli, A. Farhat, and A. Guizani, "Performance of the coupling of the flat plate collector and a heat pump system associated with a vertical heat exchanger for heating of the two types of greenhouses system," *Energy Conversion and Management*, vol. 103, pp. 266–275, 2015.

[16] R. H. E. Hassanien, M. Li, and Y. Tang, "The evacuated tube solar collector assisted heat pump for heating greenhouses," *Energy and Buildings*, vol. 169, pp. 305–318, 2018.

[17] C. Treichel and C. A. Cruickshank, "Energy analysis of heat pump water heaters coupled with air-based solar thermal collectors in Canada and the United States," *Energy*, vol. 221, article 119801, 2021.

[18] Z. Xu, J. Lu, and S. Xing, "Thermal performance of greenhouse heating with loop heat pipe solar collector and ground source heat pump," *Results in Engineering*, vol. 15, article 100626, 2022.

[19] D. Harjunowibowo, S. A. Omer, and S. B. Riffat, "Experimental investigation of a ground-source heat pump system for greenhouse heating–cooling," *International Journal of Low-Carbon Technologies*, vol. 16, no. 4, pp. 1529–1541, 2021.

[20] G. Russo, A. S. Anifantis, G. Verdiani, and G. S. Mugnozza, "Environmental analysis of geothermal heat pump and LPG greenhouse heating systems," *Biosystems Engineering*, vol. 127, pp. 11–23, 2014.

[21] G. Litjens, E. Worrell, and W. Van Sark, "Lowering greenhouse gas emissions in the built environment by combining ground source heat pumps, photovoltaics and battery storage," *Energy and Buildings*, vol. 180, pp. 51–71, 2018.

[22] N. Yildirim and L. Bilir, "Evaluation of a hybrid system for a nearly zero energy greenhouse," *Energy Conversion and Management*, vol. 148, pp. 1278–1290, 2017.

[23] M. Ebrahimi and A. Keshavarz, *Combined Cooling, Heating and Power: Decision-Making, Design and Optimization*, Elsevier, 2015.

[24] C. G. Lee, L. H. Cho, S. Park et al., "Smart farm heating using a hybrid pellet boiler–hydrothermal heat pump system," *Journal of Biosystems Engineering*, vol. 47, no. 2, pp. 233–247, 2022.

[25] I. R. Cristóbal-Monreal and R. Dufo-López, "Optimisation of photovoltaic-diesel-battery stand-alone systems minimising system weight," *Energy Conversion and Management*, vol. 119, pp. 279–288, 2016.

[26] F. Odoi-Yorke, J. J. Owusu, and L. Atepor, "Composite decision-making algorithms for optimisation of hybrid renewable energy systems: port of Takoradi as a case study," *Energy Reports*, vol. 8, pp. 2131–2150, 2022.

[27] T. Maatallah, S. El Alimi, and S. B. Nassrallah, "Performance modeling and investigation of fixed, single and dual-axis tracking photovoltaic panel in Monastir city, Tunisia," *Renewable and Sustainable Energy Reviews*, vol. 15, no. 8, pp. 4053–4066, 2011.

[28] G. Ciulla, V. Lo Brano, and E. Moreci, "Forecasting the cell temperature of PV modules with an adaptive system," *International Journal of Photoenergy*, vol. 2013, Article ID 192854, 10 pages, 2013.

[29] Canadian Solar[cited 2022 02 October], https://www.csisolar.com/bihiku7/.

[30] S. Kujak and K. Schultz, "Compositional Fractionation Studies of R410A Alternative R452B or DR55 and Their Impact on Flammability Behavior and Safety Implications," in *16th International Refrigeration and Air Conditioning Conference at Purdue*, West Lafayette, IN, USA, July 2016.

[31] Ö. Ç. Mutlu and T. Zeng, "Challenges and opportunities of modeling biomass gasification in Aspen Plus: a review," *Chemical Engineering & Technology*, vol. 43, no. 9, pp. 1674–1689, 2020.

[32] D. H. Kim, H. S. Park, and M. S. Kim, "The effect of the refrigerant charge amount on single and cascade cycle heat pump systems," *International Journal of Refrigeration*, vol. 40, pp. 254–268, 2014.

[33] S. Moritani and A. Akahira, "Influence of parameters on the estimation of coefficient of performance for R410a refrigerant," *International Journal of Thermophysics*, vol. 41, no. 9, pp. 1–17, 2020.

[34] F. Guo, Y. Dong, L. Dong, and C. Guo, "Effect of design and operating parameters on the gasification process of biomass in a downdraft fixed bed: an experimental study," *International Journal of Hydrogen Energy*, vol. 39, no. 11, pp. 5625–5633, 2014.

[35] A. Elorf and B. Sarh, "Excess air ratio effects on flow and combustion caracteristics of pulverized biomass (olive cake)," *Case Studies in Thermal Engineering*, vol. 13, article 100367, 2019.

[36] A. Quintero-Marquez, C. Bernard, A. Zoulalian, and Y. Rogaume, "Improving the operation of an automatic wood chip boiler by optimizing CO emissions," *Energy & Fuels*, vol. 28, no. 3, pp. 2152–2159, 2014.

[37] K. Rabea, S. Michailos, M. Akram, K. J. Hughes, D. Ingham, and M. Pourkashanian, "An improved kinetic modelling of woody biomass gasification in a downdraft reactor based on the pyrolysis gas evolution," *Energy Conversion and Management*, vol. 258, article 115495, 2022.

[38] J. Lu, W. Wang, Y. Zhang, and S. Cheng, "Multi-objective optimal design of stand-alone hybrid energy system using entropy weight method based on HOMER," *Energies*, vol. 10, no. 10, p. 1664, 2017.

[39] D. Coppitters, W. De Paepe, and F. Contino, "Robust design optimization of a photovoltaic-battery-heat pump system with thermal storage under aleatory and epistemic uncertainty," *Energy*, vol. 229, article 120692, 2021.

[40] F. Odoi-Yorke, S. Abaase, M. Zebilila, and L. Atepor, "Feasibility analysis of solar PV/biogas hybrid energy system for rural electrification in Ghana," *Cogent Engineering*, vol. 9, no. 1, p. 2034376, 2022.

[41] I. Dimitriou, H. Goldingay, and A. V. Bridgwater, "Techno-economic and uncertainty analysis of biomass to liquid (BTL) systems for transport fuel production," *Renewable and Sustainable Energy Reviews*, vol. 88, pp. 160–175, 2018.

[42] S. Michailos, M. Walker, A. Moody, D. Poggio, and M. Pourkashanian, "Biomethane production using an integrated anaerobic digestion, gasification and CO_2 biomethanation process in a real waste water treatment plant: a techno-economic assessment," *Energy Conversion and Management*, vol. 209, article 112663, 2020.

[43] S. Michailos, S. McCord, V. Sick, G. Stokes, and P. Styring, "Dimethyl ether synthesis via captured CO2 hydrogenation within the power to liquids concept: a techno-economic

assessment," *Energy Conversion and Management*, vol. 184, pp. 262–276, 2019.

[44] IEA, *Renewables 2019: Market Analysis and Forecast from 2019 to 2024*, IEA, 2019.

[45] N. Lamaison, S. Collette, M. Vallée, and R. Bavière, "Storage influence in a combined biomass and power-to-heat district heating production plant," *Energy*, vol. 186, article 115714, 2019.

[46] M. Dahl, A. Brun, and G. B. Andresen, "Cost sensitivity of optimal sector-coupled district heating production systems," *Energy*, vol. 166, pp. 624–636, 2019.

[47] J. Chau, T. Sowlati, S. Sokhansanj, F. Preto, S. Melin, and X. Bi, "Techno-economic analysis of wood biomass boilers for the greenhouse industry," *Applied Energy*, vol. 86, no. 3, pp. 364–371, 2009.

[48] V. I. Heating, "Reventon fan coil unit heater farmer," 2022, https://www.vpsindustrialheating.co.uk/product/fan-coil-unit-heater-farmer/.

[49] J. Ikäheimo, E. Pursiheimo, J. Kiviluoma, and H. Holttinen, "Role of power to liquids and biomass to liquids in a nearly renewable energy system," *IET Renewable Power Generation*, vol. 13, no. 7, pp. 1179–1189, 2019.

[50] A. R. Espagnet, *Techno-Economic Assessment of Thermal Energy Storage Integration into Low Temperature District Heating Networks*, KTH School of Industrial Engineering and Management, Stockholm, Sweden, 2016.

[51] Y. F. Baba, H. Ajdad, A. Al Mers, A. Bouatem, B. B. Idrissi, and S. El Alj, "Preliminary cost-effectiveness assessment of a linear Fresnel concentrator: case studies," *Case Studies in Thermal Engineering*, vol. 22, article 100730, 2020.

[52] H. Niaz, M. M. Lakouraj, and J. Liu, "Techno-economic feasibility evaluation of a standalone solar-powered alkaline water electrolyzer considering the influence of battery energy storage system: a Korean case study," *Korean Journal of Chemical Engineering*, vol. 38, no. 8, pp. 1617–1630, 2021.

[53] C. Brandoni, N. N. Shah, I. Vorushylo, and N. J. Hewitt, "Polygeneration as a solution to address the energy challenge of an aging population," *Energy Conversion and Management*, vol. 171, pp. 635–646, 2018.

[54] B. Goldstein, G. Hiriart, R. Bertani et al., "Geothermal energy," in *Renewable Energy Sources and Climate Change Mitigation: Special Report of the Intergovernmental Panel on Climate Change*, Cambridge, 2012.

[55] G. Chiriboga, S. Capelo, P. Bunces et al., "Harnessing of geothermal energy for a greenhouse in Ecuador employing a heat pump: design, construction, and feasibility assessment," *Heliyon*, vol. 7, no. 12, article e08608, 2021.

[56] A. Casasso, P. Capodaglio, F. Simonetto, and R. Sethi, "Environmental and economic benefits from the phase-out of residential oil heating: a study from the Aosta Valley region (Italy)," *Sustainability*, vol. 11, no. 13, p. 3633, 2019.

[57] H. Dorotić, T. Pukšec, and N. Duić, "Analysis of displacing natural gas boiler units in district heating systems by using multi-objective optimization and different taxing approaches," *Energy Conversion and Management*, vol. 205, article 112411, 2020.